ISSN 1726-5479

SENSORS & TRANSDUCERS

vol. 108
9/09

IEEE

TEDS Sensors, IEEE 1451 Standards

International Frequency Sensor Association Publishing

IFSA

Sensors & Transducers

Volume 108, Issue 9
September 2009

www.sensorsportal.com

ISSN 1726-5479

Sensors & Transducers Journal (ISSN 1726-5479) is a peer review international journal published monthly online by International Frequency Sensor Association (IFSA).
Available in electronic and on CD.

Sensors & Transducers Journal

Contents

Volume 108
Issue 9
September 2009

www.sensorsportal.com

ISSN 1726-5479

Research Articles

Authors are encouraged to submit article in MS Word (doc) and Acrobat (pdf) formats by e-mail: editor@sensorsportal.com
Please visit journal's webpage with preparation instructions: http://www.sensorsportal.com/HTML/DIGEST/Submition.htm

Sensors & Transducers Journal, Vol. 108, Issue 9, September 2009, pp. 102-115

www.sensorsportal.com

Sensors & Transducers

ISSN 1726-5479

http://www.sensorsportal.com

Time Domain Analysis of Ultrasonic Wave Propagation Using an Electromagnetic Acoustic Transducer

[1]Sadiq THOMAS, [1]Salah OBAYYA, [1]Domenico PINTO, [2]D. DULAY, [3]W. BALACHANDRAN, [4]Mostafa DARWISH

[1]Faculty of Advanced Technology, University of Glamorgan, Pontypridd CF37 1DL, Wales, UK
[2]NDT consultants limited, Middlemarch house, siskin drive, Coventry, CV3 4FJ, UK
[3]School of Engineering and Design, Brunel University, Uxbridge, UB8 3PH, UK
[4] University of Wales Newport, Newport, UK
[1]Tel.: +44 (0) 1443 483 490, fax: +44 (0) 1443 654 087
E-mail: sobayya@glam.ac.uk

Received: 24 July 2009 /Accepted: 21 September 2009 /Published: 28 September 2009

Abstract: In this paper an Electromagnetic Acoustic Transducer (EMAT) transmitter and receiver system is modelled. This work uses finite element as the numerical method to efficiently calculate the EMAT model. The model is capable of solving the transmitting and receiving of ultrasonic waves in non ferromagnetic materials. The EMAT model accounts for the coupling of electromagnetic analysis, mechanical analysis and acoustic analysis. The Finite element method used was thoroughly investigated by varying the mesh density and time step for convergence test and the EMAT parameters such as Rayleigh damping were also investigated to efficiently produce accurate results. The presented model also accounts for the calculation of induced voltage at the receiving EMAT by converting the transient particle displacement field in the aluminium material, and a shear stress analysis was conducted at different depths in the material. *Copyright © 2009 IFSA.*

Keywords: EMAT, Finite element modelling, Nondestructive testing, Ultrasonic testing, Wave propagation

1. Introduction

Electromagnetic Acoustic Transducer (EMAT) is an emerging technology that provides a non-contact process of testing materials compared to Ultrasonic Testing (UT) technique that requires a coupling

medium [1]. EMAT consists of a permanent magnet or electromagnet, meander coils and a conductive material as shown in Fig. 1a. The meander coils are placed underneath the magnet near the surface of the conducting materials, and excited by an external current at a desired frequency. This leads to induced current at the skin depth surface of the electrical conducting material [2]. The interaction between induced current and static magnetic fields creates a force known as the Lorentz force which excites the material to generate ultrasonic acoustic waves. This wave propagates through material and can be detected by the receiving EMAT, as shown in Fig. 1b.

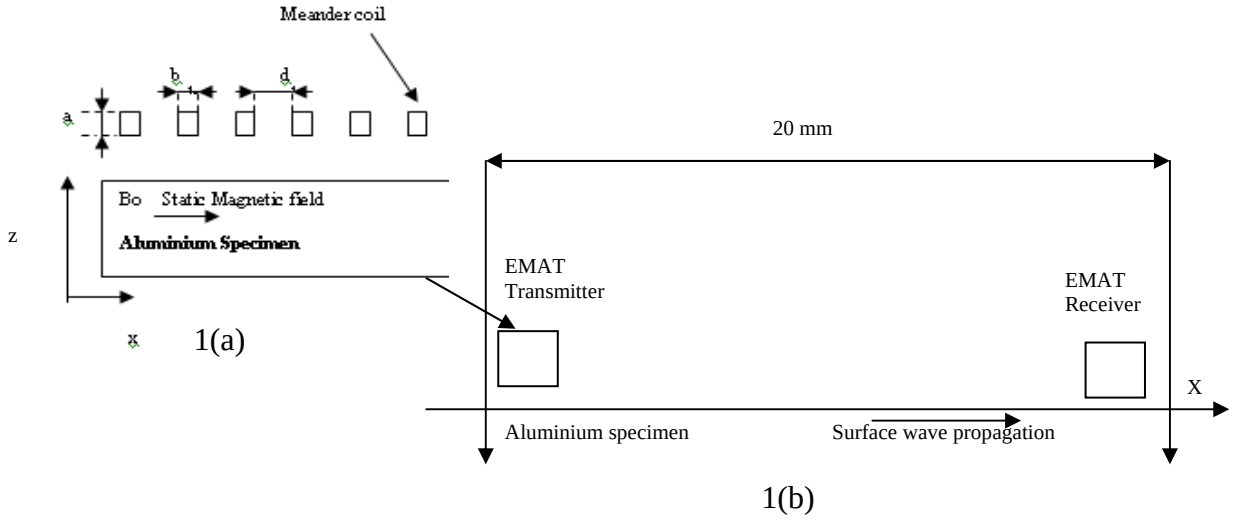

Fig. 1. (a) Two dimensional EMAT transmitter configuration; (b) EMAT transmitter receiver configuration.

An advantage of EMAT over UT method is that no direct contact is needed between the EMAT device and the material under testing. For this reason it can be used for testing hot materials, materials covered by a layer of rust, or even testing moving materials. EMAT can also be configured easily to excite ultrasonic pulse in any direction in a material. It is also easier to excite Shear Horizontal wave which is hard to achieve using piezoelectric transducers [3]. There are several types of forces that EMAT generates to excite the material depending on the material properties. Lorentz force is used to excite non-ferromagnetic material, such as aluminium, to generate wave propagation. While with ferromagnetic materials, such as steel, additional forces need to be considered, theses are known as magnetostriction and magnetization forces [1]. A major disadvantage of using EMAT is the poor signal to noise ratio (SNR). This is caused by the poor efficiency of the transduction effect in both the transmitter and receiver [3]. The design of an EMAT transmitter/receiver system should be optimized to produce the best possible signal to noise ratio (SNR). In [4] a technique has been used to compensate for the poor SNR, where the electrical impedance of the system components is carefully matched to minimize the loss of signal. In general, work carried out on the design of EMAT is done by trail and error or semi-experimental procedures [3]. In [5] Thompson an experimental work has been conducted to achieve the best SNR for different inspection tasks, a model for generation of lamb waves with an EMAT was developed. While Ludwig el al. [6] and Kaltenbacher, et. al [7], [8] focused on numerical model, which is based on finite element and finite difference methods for testing non ferromagnetic material. The emphasis in Kaltenbacher work was based on guided wave generation and reception in thin plate. Mirkhani, et. al [3] work was based on experimental and numerical methods of analyzing an EMAT transmitter, where the EMAT model gives several important improvements over previous published work. This work includes, spatial inhomogeneities in the magnetic flux density are calculated and used to determine the body force. Xjian, et. al [9], [10] worked on Raleigh wave and the effect on ultrasonic generation of a back plate in EMATs. Where a permanent magnet is included

behind the EMAT coils and an electrically conducting backplate is placed between the coil and the magnet to prevent ultrasonic generation in the magnet by the current generated in the EMAT coil. Shapooradadi [11], [12] also presented finite element analysis of EMATs operating in transmitting mode, where two different definitions of source current density are compared to highlight the importance of skin and proximity effects. Ludwig et. al [13] developed a multi-stage numerical model of an EMAT system, particular focusing on the EMAT receiver. The model is capable of accounting for static magnetic field, pulsed eddy current, Lorentz force distribution, acoustic wave generation and propagation and acoustic wave detection. This work also focuses on the conversation of the transient particle displacement fields into an induced voltage response as part of EMAT receiver system.

The main objective of this paper is to develop an EMAT transmitter/receiver system to investigate the wave propagation between transmitter and the receiver. The investigation includes the analysis of the external current density, the induced current density at the surface of the material, the calculation of the magnetic vector potential of both scenarios and the coupling of the electromagnetic and the mechanical analysis. Also rigorous convergence test for the stability of the finite element model were conducted and thorough investigation on how the Rayleigh damping [14] parameters affect the mechanical vibration in the material. The presented numerical model has been developed in the spirit of [13], to accurately account for the conversion of the transient particle displacement fields into induced voltage in the transmitting and receiving coils, also accounts for surface wave propagation in the aluminum material and shear stress at different depth in material.

2. Analysis

The governing equation involved in transient magnetic field for the transmitting EMAT as shown in Fig. 1a, is expressed in terms of magnetic vector potential (MVP) *A*, and source current density (SCD). The current density J_{sk}, s_k is the cross section area of the k_{th} source conductor and MVP A_z have only Z-component, assuming the material is infinity long [11],

$$-div\frac{1}{\mu}gradA_z + \sigma\frac{\partial A_z}{\partial t} = J_{sk}\,, \tag{1}$$

where σ is the conductivity, A_z is the Z-component of the MVP, and μ is the permeability, J_{sk} is the SCD of the *K-th* source conductor.

For the geometry of the system shown in Fig. 1a, a simple expression for the source current density J_{sk} can be used, as expressed below

$$J_{sk} = \frac{i_k(t)}{S_k}\,, \tag{2}$$

where $i_k(t)$ is the total current flowing in the K-th source coil conductor, and S_k is the cross section area of the coil conductor. Substituting Eq.(2) in Eq.(1), the governing equation for the transient magnetic field of the transmitting EMAT becomes

$$-div\frac{1}{\mu}gradA_z + \sigma\frac{\partial A_z}{\partial t} = \frac{i_k(t)}{S_k} \tag{3}$$

To further improve the accuracy of the equation (3) the effects of the magnetic field generated in the coils is taken into account and this increases the accuracy when modelling the real phenomenon. To

achieve this, the integral form of Maxwell equations is used to insert the effect of the magnetic field generated in the coils in the expression of J_{sk}, which leads to:

$$J_{sk} = \frac{i_k(t)}{S_k} + \frac{\sigma}{S_k}\frac{\partial}{\partial t}\iint_{R_k} A_z ds \tag{4}$$

J_{sk} is the function of total current and the time derivatives of the surface integral of the magnetic vector potential (A_z) [11], where R_k represents the cross-section region of the *K-th* conductor. By substituting Eq.(4) into Eq.(1), the following equation is obtained

$$-div\frac{1}{\mu}gradA_z + \sigma\frac{\partial A_z}{\partial t} - \frac{\sigma}{S_k}\frac{\partial}{\partial t}\iint_{R_k} A_z ds = \frac{i_k(t)}{S_k} \tag{5}$$

In this equation the magnetic fields produced by the coils are taken into account, which gives an accurate equation for modelling the transmitting section.

$$\sigma \mathrm{T}\frac{d\mathrm{A}}{dt} + \frac{1}{\mu}\mathrm{SA} = \mathrm{TJ}_s \tag{6}$$

Eq.(6) is then discretized using a Finite element procedure in the whole computation domain obtaining [12], [14]**, w**here **A** and matrices $\mathbf{S}_{\mathrm{n\ x\ n}}$ and $\mathbf{T}_{\mathrm{n\ x\ n}}$ are FE coefficient matrices [12], [15].
Same procedure if followed for Eq.(6), obtaining

$$\sigma(\mathrm{T} - \mathrm{QP}^{-1}\mathrm{Q}^T)\frac{d\mathbf{A}}{dt} + \frac{1}{\mu}\mathrm{SA} = \mathrm{QP}^{-1}I(t) \tag{7}$$

To solve the ordinary differential equation (8), a pure implicit scheme is applied [12]

$$\left(\frac{\mathrm{R}}{\Delta t} + \frac{1}{\mu}\mathrm{S}\right)\mathrm{A}_n = \frac{\mathrm{R}}{\Delta t}\mathrm{A}_{n-1} + \mathrm{QP}^{-1}I(t_n), \tag{8}$$

where the matrix $\mathbf{R}_{\mathrm{n\ x\ n}}$ is giving by

$$\mathrm{R} = \sigma(\mathrm{T} - \mathrm{QP}^{-1}Q^T) \tag{9}$$

and **R** is symmetric [12]

The Lorentz force in the material is calculated as the aluminium material has no magnetization properties. The Lorentz force is a result of the interaction between the induced current J_z and the magnetic flux density B_o .The calculation of the interaction between these fields is conducted, leading to the force component being calculated. [3]

$$\vec{f}_L = \vec{J} \times \vec{B}_0 \tag{10}$$

The direction of the force is also determined by Eq.(10). Due to the set up of the 2D EMAT model, B_0 has *x* and *y* components, while induced current J_z has only one component in *z* direction.

The Lorentz force calculated above is coupled with the mechanical analysis to vibrate the material which launches the acoustic wave in the material. The acoustic field equation is stated in terms of a particle displacement vector $\vec{\mu}$ and the Lorentz force as follows

$$\mu\nabla\times\nabla\times\vec{\mu}-(\lambda+2\mu)\nabla\nabla.\vec{\mu}+p\frac{\partial^2\vec{\mu}}{\partial t^2}=\vec{f}_L, \tag{11}$$

where ρ is mass volume density and λ and μ are lame constants [11], [15].

Following the thoroughly investigated Transmitting EMAT, the Receiving EMAT case is now analyzed. The incoming acoustic wave forms an angle at the receiving EMAT with respect to z axis, B_0(y,z) is a static magnetic flux density, *v*(y,z,t) is the particle velocity and σ is the conductivity of the specimen [13]. A free conducting current density distribution *J* is formed at the surface of the specimen under the receiving EMAT due to the mechanical vibrations in the material and the presence of a static magnetic field [13].

$$J=\sigma V\times B_0 \tag{12}$$

This leads to a time varying magnetic vector potential A(y, z, t) in and around the specimen underneath the receiving EMAT which can be detected as a voltage in the receiving pick up coils.

Damping is important in time dependent EMAT analysis, a common model for damping is known as Rayleigh damping, where the damping is assumed to be proportional to a linear combination of the stiffness and the mass. Using the Comsol software tool [14], the damping parameter *c* is expressed in terms of the mass and the stiffness *k*

$$c=\alpha_{dM}m+\beta_{dK}k, \tag{13}$$

where α_{dM} is the mass and β_{dK} is the stiffness damping parameters.

This leads to investigating the Rayleigh damping parameter for the aluminium material under test. Obtaining the appropriate damping parameter can be a problem [13]. A more physical damping measure is the damping ratio, which is the ratio between the actual and critical damping. It is possible to transform damping factors to Rayleigh damping parameters. For a specified damping factor ξ as a frequency *f*

$$\xi=\frac{1}{2}\left(\frac{\alpha_{dM}}{2\pi f}+\beta_{dK}2\pi f\right) \tag{14}$$

This relationship is used at two frequencies f_1 and f_2 with different damping factor ξ_1 and ξ_2, which results in an equation system.

$$\begin{bmatrix}\frac{1}{4\pi f_1}\pi f_1\\ \frac{1}{4\pi f_2}\pi f_2\end{bmatrix}\begin{bmatrix}\alpha_{dM}\\ \beta_{dK}\end{bmatrix}=\begin{bmatrix}\xi_1\\ \xi_2\end{bmatrix} \tag{15}$$

Using the same damping factor ξ_1 and ξ_2 does not result to the same damping factors in the interval. To get the appropriate damping parameters for this EMAT model, two values for the frequencies was varied according to the centre frequency of this model of 1.8 MHz.

Fig. 2 shows the first pick up coil of six coils above the specimen. To calculate the voltage in the receiving pick up coils, the first step is to calculate transient particle displacement in the material, leading to the second stage, which is to use the result as a source term to calculate the MVP (A_z) around the receiving coils. After solving for A_z around the receiving coils, the third stages requires a numerical method for the calculation of the induced voltage (emf) in the coil in equation (15). This is based on the evaluation of the faraday law which relates the induced emf to the flux density B. For a finite cross sectional one coil (Fig. 2), the induced voltage can be defined as V_f(t), [13].

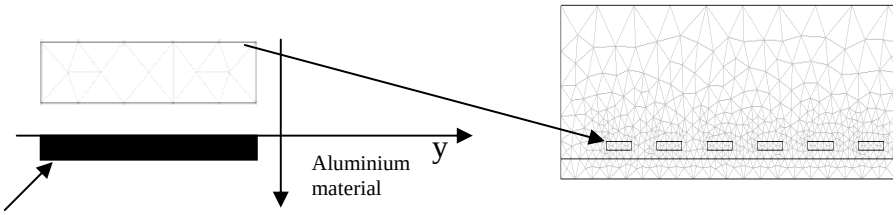

Fig. 2. Numerical representation of a finite cross section one turn picks up coil, with dimension 0.1 mm by 0.5 mm over a conductive material [13].

$$V_f(t) = \frac{\iint V_p(y,z,t)dydz}{\iint dydz}, \tag{16}$$

where the voltage V_p (y, z, t) due to a point pick up coil is given by

$$V_p(y,z,t) = -\frac{\partial}{\partial t}\iint B.ds$$

$$= -\frac{\partial}{\partial t}\iint (\nabla \times A).dS = -\int_c \frac{\partial A}{\partial t}.dl \tag{17}$$

Equation (13) signifies the total point contribution average over the cross sectional area of the finite size coil[13]. The finite evaluation of (13) leads to the numerical expression

$$V_f(t+\Delta t) = -\frac{\sum_{i-1}^{M} \frac{y_{ci}}{\Delta t}[A_{ci}(t+\Delta t) - A_{ci}(t)]}{\sum_{i=1}^{M} \Delta_i} \tag{18}$$

Δ_i is the area i^{th} triangular element, y_{ci} is centrodial distance, and A_{ci} is the centroidal vector potential value as shown in Fig. 2, the summation extends over all the source elements comprising the probe [13].

3. Results

Before proceeding to the analysis of wave propagation between the transmitting and receiving EMAT, analysis will initially be conducted on the accuracy of the model. Then the transient magnetic fields around the transmitting coils and transient particle displacement fields in the aluminium material will be calculated. This leads to the calculation of the acoustic wave propagation in the conductive material and the voltage around the transmitting and receiving coils. Fig. 1a shows the configuration of an EMAT transmitter - receiver system where both arrangements are similar, whereby the magnet is suspended over the meander coils with a few millimetre spacing between the coils and the conductive material under testing. The EMAT Transmitter/Receiver consists of a permanent magnet or electromagnet and a meander line coil with six turns suspended over a conductive material with a thickness of 0.24 mm as shown in Fig. 3. The meander coils are excited with 10 A current with a seven cycle 1.8 MHz tone burst. The coils have identical cross section of height a = 0.1 mm by width b = 0.5 mm with a wire spacing b of 0.5 mm and *lift off* of 0.1 mm, the material is immersed in a static magnetic field of 1T. It has been demonstrated in [16] that it is possible to use the interaction of the self-field of the EMAT coils with the surface eddy current to generate acoustic waves in a conductive material, which will be implemented in this scenario.

Fig. 3 shows the computational mesh of the EMAT model of 2 mm by 30 mm, which includes the aluminium material underneath the coils of 0.24 mm by 30 mm. It consists of 7697 second order mesh elements, the mesh is particularly refined around the transmitting and receiving EMAT coils as results will be extracted from these region. The mesh density will be varied in order to evaluate the accuracy of the finite element model.

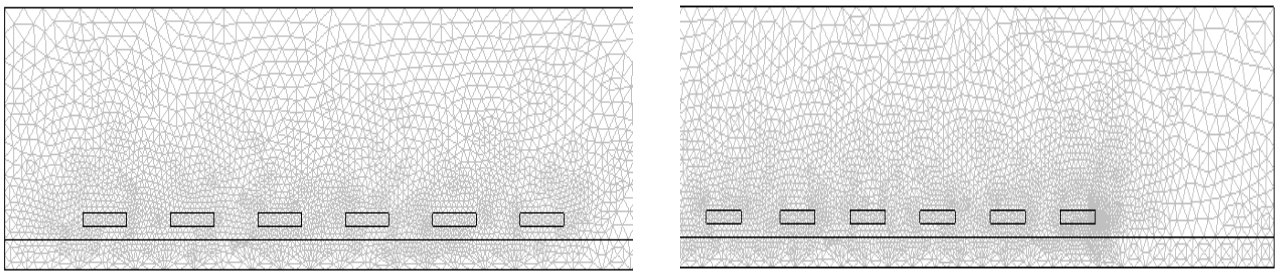

Fig. 3. EMAT Transmitter /Receiver structural Mesh consisting of 7697 second order quadratic triangular elements.

The accuracy of the numerical method is investigated by firstly decreasing the triangular mesh element size to determine the convergence of the displacement, which will ensure the convergence of all other physical quantities. A detector was placed at the surface of the material underneath the transmitting coils. The Mesh consists of second order quadratic triangular elements which are refined from 1110 to 10072 elements with Δt of 0.01 μs. Results shown in Fig.4 illustrate how the displacement reaches its convergence from 3000 elements with the.

Furthermore, the accuracy of the numerical method was tested by reducing the size of the time step. A fine mesh consisting of 7519 elements was used although results show that any amount of mesh over 3000 elements is sufficient to obtain accurate results. The detector was also placed in the same point at the surface of the material underneath the transmitting coils. By observing the result shown in Fig. 5 illustrates the time step larger than 0.1 μs is inaccurate, which is also confirmed by Nyquist law. Which fixes the lowest sampling rate that is possible to reproduce the original signal is the sample rate was (1/2f) seconds, where f is the highest frequency, in this case the largest amount of the time step to

be used in this scenario is 0.1 μs. By reducing *dt* further to 0.01 μs increased the computation running time significantly and the amplitude was further improved by 0.5 nm to the value of 4.12 nm. The running time for 0.01 μs using a 6 Gig RAM was 1521.04 s, while using 0.1 μs the running time was 120 s. The time steps were further varied between 0.01 μs and 0.05 μs to verify the size of the time step between this range results to the convergence of all physical quantities; 0.05 μs resulted to an amplitude value of 4.11 nm, 0.04 μs resulted to an amplitude value of 4.13 nm, 0.02 μs resulted to an amplitude value of 4.12 nm. Based on the results obtained from the analysis of the convergence of the model for all simulations a mesh of 7519 elements with time step size of 0.01 μs has been used.

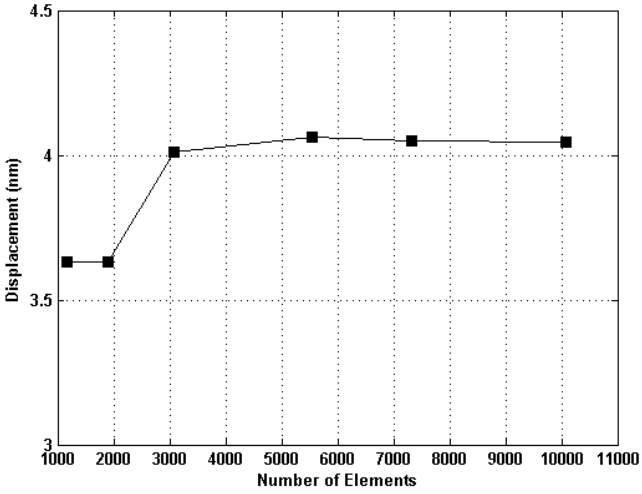

Fig. 4. Varied triangular mesh elements from coarse mesh to fine mesh.

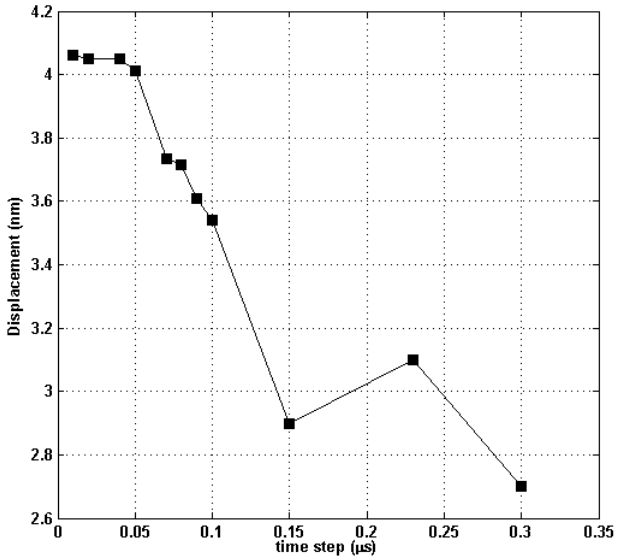

Fig. 5. Varied time step *dt* with a fine mesh of 5518 second order quadratic elements.

The transmitting EMAT scenario is analyzed first, whereby the current densities in the coils are calculated. By applying the excitation source of a seven cycle tone-burst with a centre frequency of 1.8 MHz and a current density of 10A to the coils,

$$J = I_0(\sin \omega t)[0.5(1+\cos(\omega t))] \text{ for } 0 \le t \le 4.5\mu s\,, \tag{19}$$

where J is the transient excitation current in the coils, I_o is the current amplitude =10 A and $\omega=2\pi f$ is the angular centre frequency. The material is immersed in a constant magnetic field of B_0=1T, which is used in place of the permanent magnet to produce the static magnetic field. A detector is placed in the first coil of the transmitting EMAT. Fig.6 shows the result of external current density in the coils after the excitation has been applied, showing a similarity to the seven cycle source, which proves the current density phenomenon, is dependent on the excitation source applied.

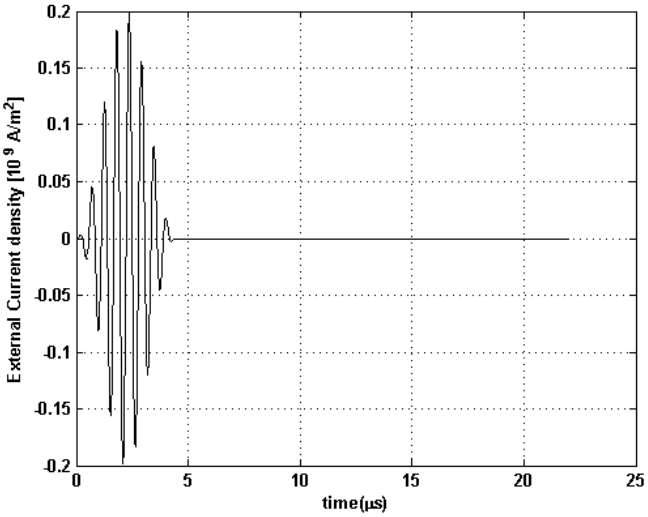

Fig. 6. The meander coil loaded with a 7 cycle 1.8 MHz tone burst signal.

Following the calculation of the external current density, the next physical quantity to be calculated is the magnetic vector potential (MVP) around the transmitting coils. The detector is placed between the coils to record the time variation of the MVP. Fig. 7 illustrates the result of the magnetic vector potential (MVP) plotted against time. The result shows the shape of the waveform is similar to the excitation applied to the coils, which proves that this phenomenon is a result of the excitation current. The calculated magnetic vector potential is used to solve the voltage around the transmitting coils as expressed in equation (18). The result shown in Fig. 8 indicates a similarity of the waveforms of the recorded voltage to the MVP, this phenomenon is expected as the voltage is a result of the MVP.

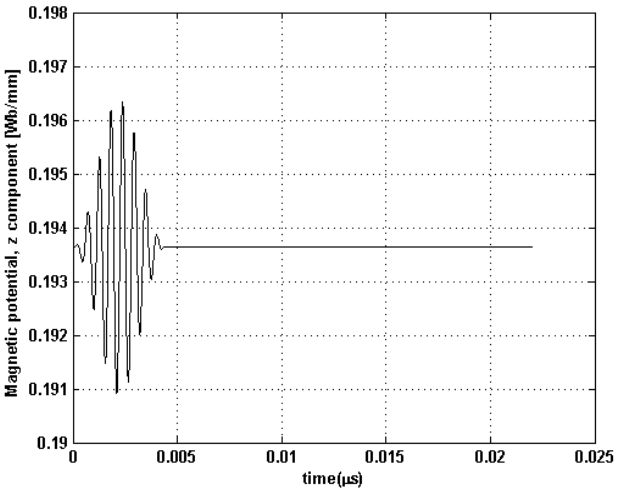

Fig. 7. Magnetic vector potential around the receiver coil.

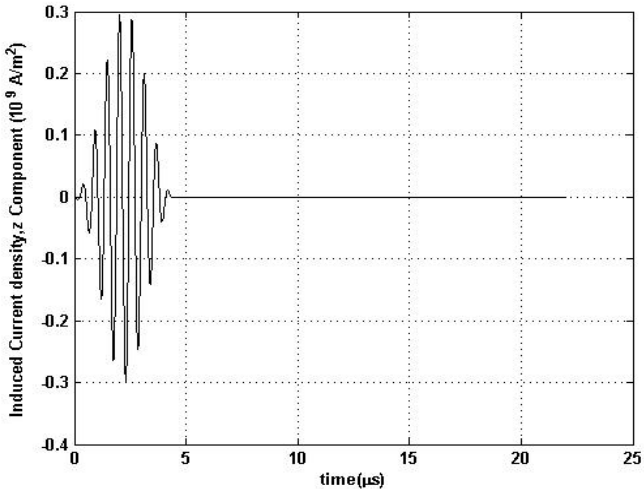

Fig. 8. Output voltage at EMAT transmitter.

Following the calculation of the transmitting voltage, the induced current at the surface of the aluminium material is the next quantity to be calculated. This is required to verify the induced current theory at the skin depth surface of the material, which will interact with the magnetic field to create Lorentz force to vibrate the material as expressed in equation (10). The detector was placed at the skin depth surface of the aluminium material (0.06 mm) underneath the transmitting coil. Fig. 9 shows the plot of the induced current z component against time, the result indicates a correlation between the excitation and the induced current as the wave forms have a similar shape. This phenomenon is expected as the induced current at the skin depth surface of the aluminium material is a result of the excitation source. The amplitude of the current density in the coil and at the surface of the material are similar, this is expected as the *lift off* of distance between the coil and the material is very small (0.1 mm).

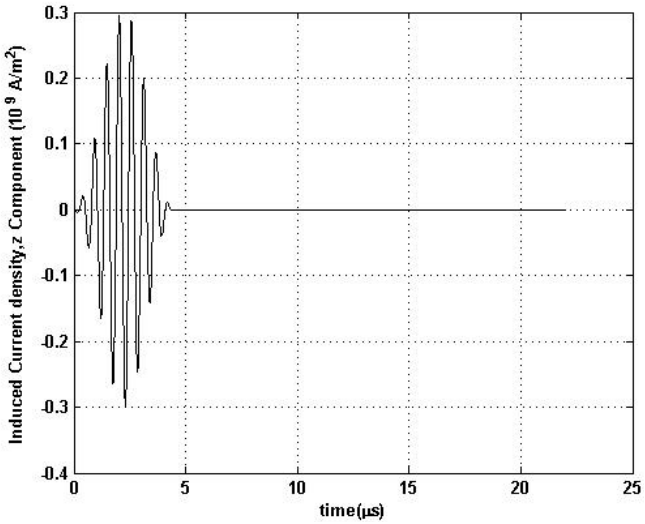

Fig. 9. Induced current at the surface of the material.

Following the analysis and the numerical computation of the transmitting EMAT, the focus is moved to the receiving part of the EMAT. In other to accurately analyze the surface wave propagation between the receiving and transmitting EMAT, certain parameters have to be taking into consideration. The parameters to investigate are the boundary conditions and Rayleigh damping of the conductive materials. Ludwig work [13] states two boundaries of the test material has to be set to free boundary conditions, which leads to the left and right boundary of the aluminium material to be set to these conditions. The next stage is to investigate the Rayleigh damping parameter for the aluminium material, as obtaining the appropriate value can be a problem [14]. In order to find the appropriate Rayleigh damping parameter value to allow the accurate surface wave propagation through the aluminium material, a physical damping measure is taking into account known as a damping ratio, which is a ratio between the actual and critical damping as expressed in equation (14). The detector is placed 20 mm away from the transmitting EMAT at the surface of the aluminium material underneath the receiving EMAT coils. The Result displayed in Fig. 10 shows the displacement at the surface of the material in x direction against time without Rayleigh damping parameters. The results prove the model permits wave propagation in the material with a delay in time of 4.5 μs. But the results also show the model is unstable as the material does not return back to its steady state. The result also affect the receiving voltage in the pick coils as shown in Fig. 11 as the calculated voltage is a result of the mechanical vibration in the material as defined in (12).

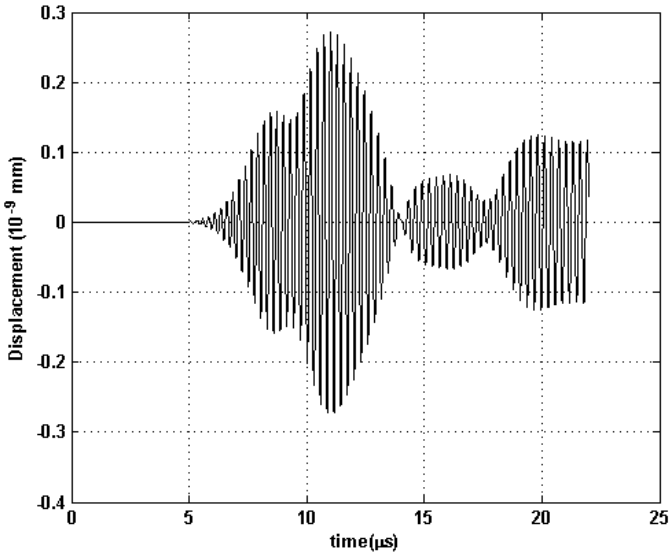

Fig. 10. Mechanical displacement in the material after 20mm without damping.

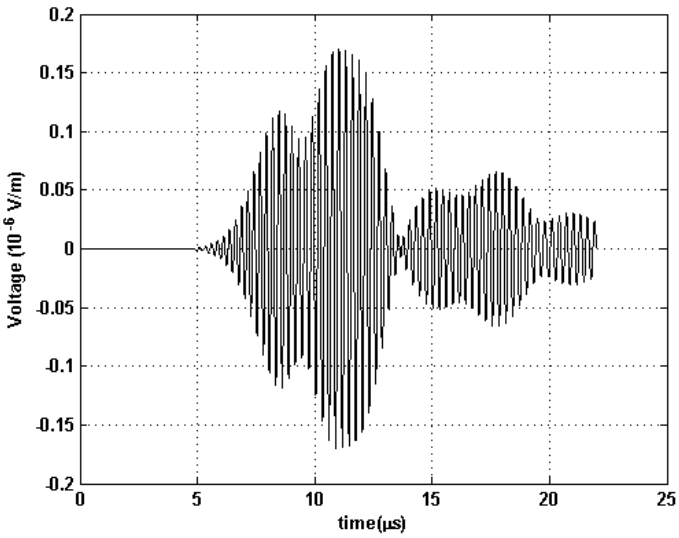

Fig. 11. Received voltage in coils without damping.

After the calculation of the appropriate damping parameters of the aluminium material with an excitation frequency of 1.8 MHz. The detector is still left at the same point 20 mm away from the transmitting EMAT. The mechanical displacement is calculated at the receiving section. The result shown in Fig. 12 indicates the model permits surface wave propagation in the aluminium material and also proves the correct damping parameters have been implemented as the model steadies after 12 μs compared to previous result shown in Fig. 11.

In order to calculate the voltage response in the receiving coils, the free current density in the material under the receiving EMAT coils has to be calculated as seen in equation (12). The free conduction current density *J* is a result of the mechanical vibration and the presence of the static magnetic field. The Results shown in Fig. 13 proves that the free conducting current present at the surface of the material is result of the mechanical displacement.

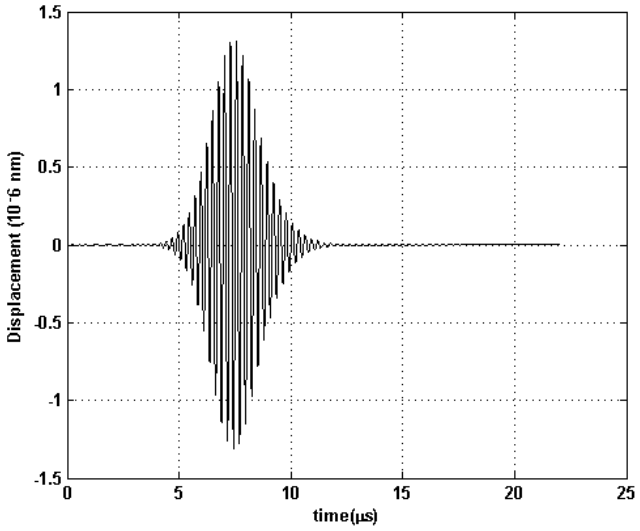

Fig. 12. Mechanical displacement in the material after 20 mm of propagation with damping.

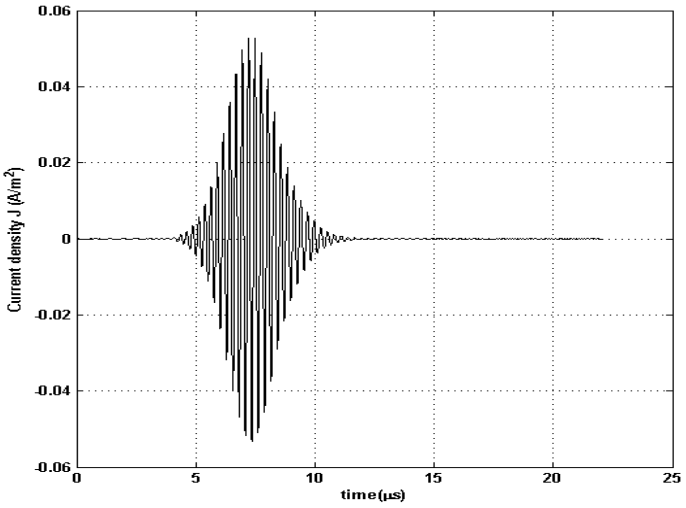

Fig. 13. Current density at the surface of the material under the receiving EMAT.

The current density formed inside the material is used to calculate the magnetic vector potential around the receiving coils. Following the calculation of the magnetic vector, the voltage is calculated from the resulting MVP using the derived numerical equation in (18). The result shown in Fig. 14 indicates a presence of voltage around the pick coils and also records the propagation of surface wave with a time delay of 4.5 μs. There are extra cycles in the voltage result as shown in Fig. 14 compared to the seven cycle excitation, this is due to the mechanical vibration of the material and the time it takes to return to its steady state. This result agrees with already published work [7], where experiment was carried out on the receiving voltage and the additional cycles where recorded at the receiving end compared to the transmitted source.

The material thickness was extended from its original thickness of 0.24 mm to 3 mm to analyze the shear stress at different depth in the material. Results shown in Fig. 15 illustrate the shear stress at the surface region of the material as a function of x, at various distance z inside the material. There is a spatial oscillation of the pulse amplitude in x direction, this is caused by the high degree of excitation

experienced by the material directly underneath each coil and the part of the material underneath the space between the coils experience less excitation. This result is in good agreements with work carried out in [3].

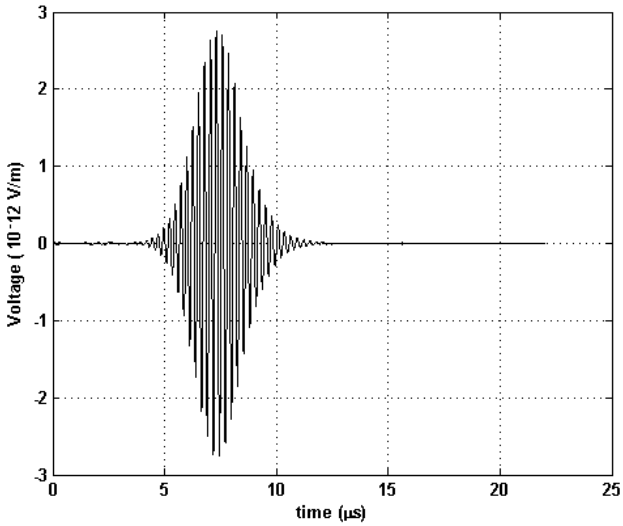

Fig. 14. Induced voltage in pick up coil.

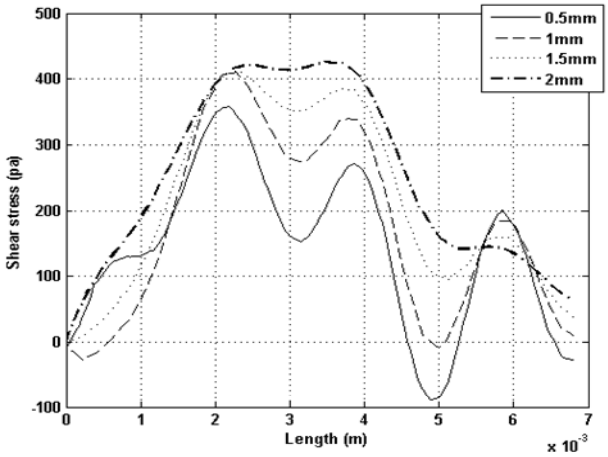

Fig. 15. Amplitude of Shear stress as a function of horizontal position x, at various depth y inside the material under the transmitting coil.

4. Conclusion

A two dimensional numerical model of an EMAT has been investigated, the model accounts for both the transmitting and receiving sections. Both cases have been studied extensively to efficiently produce optimum results; such study includes convergence test, the variation of second order quadratic triangular elements, which are already known to be very accurate for finite element method. The time steps were rigorously investigated for the efficiency of the numerical model and the appropriate damping parameters and boundary conditions that permits the efficient generation of surface ultrasonic wave. Furthermore, work was carried on the EMAT model, using the complete equation of Maxwell equation to calculate the Eddy current and Lorentz force. This leads to the calculation of the surface wave propagation in the material and the recoded transient particle displacement, which in turn is used

to calculate the induced voltage in the receiving pick up coils of the EMAT. This model can be further developed to introduce defects into the material and from the voltage measured in the pick coils results could be used to identify the presence of flaws in the material.

Acknowledgment

The work of S Thomas has been funded by The Engineering and Physical Science Research Council (EPSRC) under grant no (CASE/CNA/05/02) and also by NDT Consultants, Coventry, UK.

References

[1]. Masahiko Hirao and Hirotsugu Ogi, EMATS for SICENCE and INDUSTRY Non Contacting Ultrasonic Measurements, *Kluwer Academic Publishers*, 2003, pp. 13-64.
[2]. Tribikram Kundu, Ultrasonic Nondestructive Evaluation, *CRC Press*, 2004, pp. 495-540.
[3]. Koorosh Mirkhani, Chris Chaggares, C. Masterson et. al, Optimal design of EMAT transmitters, *NDT&E international*, Vol. 37, 2004, pp. 181 – 193.
[4]. Fortunko C. M, Schram R. E., An analysis of electromagnetic acoustic transducer arrays for nondestructive evaluation of thick material sections and weldments, *Rev Prog Quant NDE*, 2A, 2003, pp. 283-307.
[5]. Thompson R. B. Physical principles of measurement with EMAT transducers: Thuston RN, pierce AD, editors, *Physical Acoustics 19, Academics*, San Diego, 1990, p. 157 – 200.
[6]. R. Ludwig and X. W. Dai, Numerical and Analytical Modelling of Pulsed Eddy Currents in a Conduction Half-Space, *IEEE Trans. Magn*., Vol. 26, 1990, pp. 299-307.
[7]. M. Kaltenbacher, R. Lerch, H. Landes, K. Ettinger, Computer Optimization of Electromagnetic Acoustic Transducers, *IEEE Ultrasonic Symposium*, 1998, pp. 1029–1033.
[8].M. Kaltenbacher, K. Ettinger, R. Lerch and B Tittmann, Finite Element Analysis of coupled Electromagnetic Acoustic systems, *IEEE Trans. Magn*, Vol. 35, 1999, pp. 1610–1613.
[9]. X. Jian, S. Dixon, R. Edwards, K. Quirk, I. Baillie, Effects on Ultrasonic generation of a backplate in electromagnetic acoustic transducers, *Journal of Applied Physics*, July 2007.
[10].X. Jian, S. Dixon and R. Edwards, A model for pulsed Rayleigh wave and optimal EMAT design, *Journal of Applied Physics*, March 2006.
[11].R. Jafari-Shapoorabadi, A. N. Sinclair, and A. Konrad, Finite Element Determination of the Absolute Magnitude of an Ultrasonic Pulse produced by an EMAT, *IEEE Ultrasonic Symposium*, 2000, pp. 737-741.
[12].R. Jafari-Shapoorabadi, A. Konrad and A. N. Sinclair, Improved Finite Element Method for EMAT Analysis and Design, *IEEE Trans. Magn.*, Vol. 37, 2001, pp. 2821-2823.
[13].R. Ludwig, Z. You and R. Palanisamy, Numerical Simulation of an Electromagnetic Acoustic Transducer-Receiver System for NDT Applications, *IEEE Trans. Mag*., Vol. 29, 1993, pp. 2081-2089.
[14].Comsol MultiPhysics 3. 3, User Guide and Modelling library, 2006, pp. 1-164.
[15].P. P. Silvester and R. L Ferrari, Finite Elements for electrical Engineering, *Cambridge University Press*, Cambridge, UK, 1983.
[16].S. Dixon, S. B. Palmer, Wideband low frequency generation and detection of Lamb and Rayleigh waves using electromagnetic acoustic transducers (EMATs), Science direct, *Ultrasonics*, 42, March 2004, pp. 1129-1136.

Guide for Contributors

Aims and Scope

Sensors & Transducers Journal (ISSN 1726-5479) provides an advanced forum for the science and technology of physical, chemical sensors and biosensors. It publishes state-of-the-art reviews, regular research and application specific papers, short notes, letters to Editor and sensors related books reviews as well as academic, practical and commercial information of interest to its readership. Because it is an open access, peer review international journal, papers rapidly published in *Sensors & Transducers Journal* will receive a very high publicity. The journal is published monthly as twelve issues per annual by International Frequency Association (IFSA). In additional, some special sponsored and conference issues published annually. *Sensors & Transducers Journal* is indexed and abstracted very quickly by Chemical Abstracts, IndexCopernicus Journals Master List, Open J-Gate, Google Scholar, etc.

Topics Covered

Contributions are invited on all aspects of research, development and application of the science and technology of sensors, transducers and sensor instrumentations. Topics include, but are not restricted to:

- Physical, chemical and biosensors;
- Digital, frequency, period, duty-cycle, time interval, PWM, pulse number output sensors and transducers;
- Theory, principles, effects, design, standardization and modeling;
- Smart sensors and systems;
- Sensor instrumentation;
- Virtual instruments;
- Sensors interfaces, buses and networks;
- Signal processing;
- Frequency (period, duty-cycle)-to-digital converters, ADC;
- Technologies and materials;
- Nanosensors;
- Microsystems;
- Applications.

Submission of papers

Articles should be written in English. Authors are invited to submit by e-mail editor@sensorsportal.com 8-14 pages article (including abstract, illustrations (color or grayscale), photos and references) in both: MS Word (doc) and Acrobat (pdf) formats. Detailed preparation instructions, paper example and template of manuscript are available from the journal's webpage: http://www.sensorsportal.com/HTML/DIGEST/Submition.htm Authors must follow the instructions strictly when submitting their manuscripts.

Advertising Information

Advertising orders and enquires may be sent to sales@sensorsportal.com Please download also our media kit: http://www.sensorsportal.com/DOWNLOADS/Media_Kit_2009.pdf